EurJIC
European Journal of Inorganic Chemistry

Research Article
doi.org/10.1002/ejic.202100934

Chemistry Europe
European Chemical Societies Publishing

www.eurjic.org

Two Faces of the Bi–O Bond: Photochemically *and* Thermally Induced Dehydrocoupling for Si–O Bond Formation

Jacqueline Ramler,[a] Johannes Schwarzmann,[a] Andreas Stoy,[a, b] and Crispin Lichtenberg*[a, b]

The diorgano(bismuth)alcoholate [Bi($(C_6H_4CH_2)_2$S)OPh] (**1-OPh**) has been synthesized and fully characterized. Stoichiometric reactions, UV/Vis spectroscopy, and (TD-)DFT calculations suggest its susceptibility to homolytic and heterolytic Bi–O bond cleavage under given reaction conditions. Using the dehydrocoupling of silanes with either TEMPO or phenol as model reactions, the catalytic competency of **1-OPh** has been investigated (TEMPO = (tetramethyl-piperidin-1-yl)-oxyl). Different reaction pathways can deliberately be addressed by applying photochemical or thermal reaction conditions and by choosing radical or closed-shell substrates (TEMPO vs. phenol). Applied analytical techniques include NMR, UV/Vis, and EPR spectroscopy, mass spectrometry, single-crystal X-ray diffraction analysis, and (TD)-DFT calculations.

Introduction

Molecular bismuth complexes show a range of properties that turn them into highly attractive candidates for applications as catalysts in organic and inorganic reactions. This includes low costs and a good availability of starting materials, a relatively low toxicity,[1] catalyst recyclability,[2] the accessibility of cationic[3,4] and dicationic species,[5] a strong, tunable, and soft Lewis acidity,[4,6] multiple available oxidation states,[7–10] the accessibility of radical[8] and biradical species,[11] as well as the possibility to realize reversible homolytic[12] and reversible heterolytic[13] Bi–X bond cleavage (e.g.: X = Bi, C).

As a consequence, bismuth compounds with unique features have been reported as catalysts for a growing number of transformations. In Lewis acid catalysis, examples include hydroamination,[14] hydrosilylation,[5a,b] diastereoselective Mannich reactions,[15] Diels-Alder reactions,[16] and the ring-opening polymerization of cyclic esters.[17] The exploitation of Bi(I)/Bi(III) and Bi(III)/Bi(V) redox shuttling catalysis has recently allowed for reactions such as the transfer hydrogenation of azoarenes,[18] the hydrodefluorination of fluoroarenes,[19] and the fluorination of arylboronic esters to be realized.[20] In the context of main group radical chemistry,[21] bismuth catalysts have been exploited for the polymerization of activated α-olefins,[22] the cyclo-isomerization of δ-iodo-olefins,[23] and the dehydrocoupling of (2,2,6,6-tetramethylpiperidin-1-yl)oxyl (TEMPO) with silanes.[24]

With their potential to show a considerable Lewis acidity on the one hand[4,6] and low homolytic bond dissociation energies on the other hand,[8c,d,11,12,25] bismuth compounds seem to bring along the prerequisites to deliberately address different reaction pathways by complex design and the variation of reaction conditions. For example, systems that respond to photochemical and thermal activation have been investigated in the context of chemical reaction control, aiming towards the ultimate goal to synthesize different products from a pool of starting materials steered by external stimuli.[26] To the best of our knowledge, bismuth catalysts that address two different productive reaction pathways in either photochemically- or thermally-initiated transformations have not been reported to date.

Here we report the synthesis, isolation, and full characterization of a diaryl bismuth alcoholate and its catalytic activity in the photochemically- *and* thermally-initiated dehydrogenative coupling of silanes with TEMPO or phenol as model reactions.

Results and Discussion

The diaryl(bismuth)alcoholate **1-OPh** was isolated in 79% yield as a colorless solid from a salt elimination reaction of ($C_{14}H_{12}$S)BiCl with NaOPh (Figure 1a). The complex completes the series of diorgano(bismuth)chalcogenides [Bi(di-aryl)EPh] (**1-EPh**, E = O, S, Se, Te), the heavier congeners of which have

[a] Dr. J. Ramler, J. Schwarzmann, Dr. A. Stoy, Prof. Dr. C. Lichtenberg
Institute of Inorganic Chemistry,
Julius-Maximilians-University Würzburg
Am Hubland, 97074 Würzburg, Germany
[b] Dr. A. Stoy, Prof. Dr. C. Lichtenberg
Philipps-Universität Marburg,
Fachbereich Chemie
Hans-Meerwein-Str. 4, 35032 Marburg, Germany
E-mail: crispin.lichtenberg@chemie.uni-marburg.de

Supporting information for this article is available on the WWW under https://doi.org/10.1002/ejic.202100934

Part of a joint Special Collection on "Main Group Catalysis". Please click here for more articles in the collection.

Research Article
doi.org/10.1002/ejic.202100934

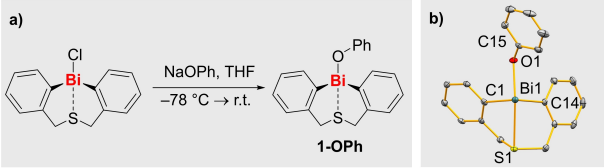

Figure 1. Synthesis (a) and molecular structure in the solid state (b) of compound **1-OPh**. Displacement parameters are drawn at the 50% probability level. Selected bond lengths (Å) and angles (°): Bi1–C1, 2.263(3); Bi1–C14, 2.249(3); Bi1–O1, 2.2176(18); Bi1–S1, 2.8995(7); C1–Bi1–C14, 97.25(9); C1–Bi1–O1, 89.27(8); C14–Bi1–O1, 85.99(8); S1–Bi1–O1, 151.49(5).

recently been investigated as catalysts in the dehydrocoupling of phenylsilane with TEMPO.[24]

Single-crystal X-ray diffraction analysis of **1-OPh** revealed a typical molecular structure without directional intermolecular bonding in the solid state (Figure 1b, orthorhombic space group *Pbca* with $Z=8$). The Bi1–O1 distance of 2.22 Å and the Bi–C1/14 distances of 2.25–2.26 Å lie in the range of bond lengths reported for the small number of literature-known mononuclear diorgano bismuth(III) alcoholates (Bi–O: 2.13–2.33 Å; Bi–C: 2.17–2.31).[27] The bisphenoidal coordination geometry of the central bismuth atom in **1-OPh** is commonly found for bismuth atoms with a coordination number of four, with the carbon-based ligands in the equatorial positions.[5c,28] A detailed comparison of compounds **1-EPh** (E = O–Te) uncovered a close relationship of the structural parameters within this series of compounds (Table 1).[29]

Bonding interactions between Bi1 and the sulphur atom S1 are present in all these complexes.[23a,24b] The Bi1–S1 distance steadily increases with a growing atomic number of E. This is due to the electronegativity of E decreasing in the same order, thus resulting in the most polarized Bi–E bond and the shortest Bi1–S1 distance in **1-OPh**. Accordingly, the Bi–C bond lengths in **1-OPh** are on average and within one standard deviation the shortest ones among compounds **1-EPh**. This was also ascribed to the high electronegativity of oxygen, which leads to a relatively high partial charge at bismuth.

The bonding situation in compound **1-OPh** was investigated by density functional theory (DFT) calculations and natural bond orbital (NBO) analyses at the B3LYP/LANL2DZ (Bi), 6-31G(d,p) (H, C, O, S) level of theory, i.e. at the same level of theory as the remaining compounds in the series **1-EPh**. According to NBO analyses, the Bi–O bond in **1-OPh** is realized through a n(O1)→p(Bi) interaction with a deletion energy of 92.1 kcal·mol^{-1}. The natural charge at the bismuth atom amounts to +1.46. This is in contrast to the bonding situation in **1-EPh** with E = S–Te, where NBO analyses indicate covalent σ-type Bi–EPh bonding and natural charges at the bismuth atoms of +1.21 (E = S), +1.13 (E = Se), and +1.03 (E = Te).[24b] As a result, the S1–Bi1 interaction originates either from n(S1)→p(Bi) interactions (E = O) or from n(S1)→σ*(Bi–EPh) bonding (E = S–Te). Despite the qualitative differences in Bi–S bonding according to NBO theory, the deletion energies for these interactions are similar to each other with **1-OPh** showing the largest value (E = O: 21.7 kcal·mol^{-1}; E = S–Te: 18.2–21.3 kcal·mol^{-1}).[24b]

The ^{1}H NMR spectroscopic analysis of **1-OPh** in solution revealed two characteristic doublets for the protons in benzylic positions and typical ABCD and A_2B_2C signal patterns for the benzo and the phenyl group, respectively. The protons at the α-carbon atoms (relative to the C–Bi functional group) characteristically resonate at high frequencies (δ = 8.80 ppm), albeit this effect is less pronounced than for compounds **1-EPh** (δ = 9.34 (E = S), 9.40 (E = Se), 9.48 (E = Te) ppm).[23a,24b] The ^{13}C NMR chemical shifts of the bismuth-bound carbon atoms in **1-EPh** nicely reflect the trends of the natural charges at the bismuth atom, thus resulting in the highest chemical shift for the Bi–*C* atoms in **1-OPh**: δ = 176.8 (E = O), 165.1 (E = S), 161.1 (E = Se), 154.5 (E = Te) ppm.[23a,24b]

In order to evaluate the potential of **1-OPh** for photochemically induced reactions, UV/Vis spectroscopy in combination with (TD)-DFT calculations were conducted with the CAM–B3LYP functional and the same basis sets as for the DFT calculations. The experimental UV/Vis spectrum of **1-OPh** in acetonitrile solution shows an absorption feature beginning at ca 350 nm (Figure 2). Due to significant overlap with solvent absorptions in the UV region, experimental absorption maxima are only tentatively assigned at λ_{max}(exp) = 261 nm and λ_{max}(exp) = 269 nm. According to TD-DFT calculations the absorption corresponds to two singlet-singlet transitions at λ_{max}(theo)-

Table 1. Selected bond parameters in species **1-EPh** (E = O, S, Se, Te), as determined by single-crystal X-ray analyses.

Bonding parameter	**1-OPh**	**1-SPh**[23a]	**1-SePh**[24b]	**1-TePh**[24b]
Bi–E [Å]	2.2176(18)	2.6149(16)	2.7285(11)	2.9296(3)
Bi–S [Å]	2.8995(7)	2.9401(15)	2.966(3)	3.0007(7)
Bi–C [Å]	2.263(3),	2.254(5),	2.284(11),	2.288(3),
[average]	2.249(3)	2.287(5)	2.303(10)	2.289(3)
	[2.256(3)]	[2.271(5)]	[2.294(11)]	[2.289(3)]
S–Bi–E [°]	151.49(5)	157.10(4)	157.23(6)	161.818(14)

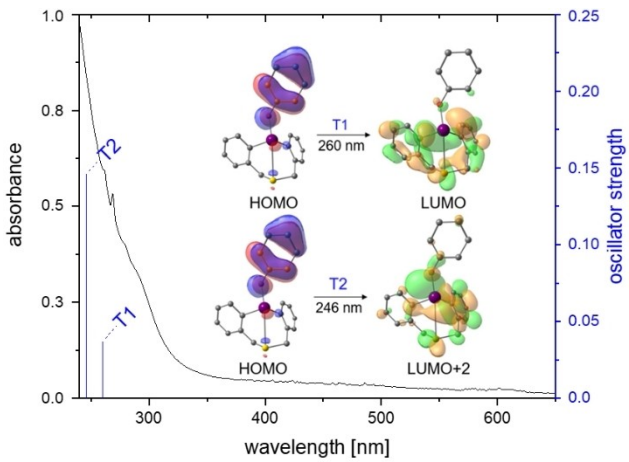

Figure 2. Experimental UV/Vis spectrum of **1-OPh** in acetonitrile at a concentration of $c = 0.78$ mmol·L^{-1} (solid black line), lowest energy calculated transitions (blue bars), and molecular orbitals involved in the two lowest calculated absorptions. Isovalue = 0.03.

Research Article
doi.org/10.1002/ejic.202100934

= 260 (T1) and λ_{max}(theo) = 246 nm (T2). T1 and T2 correspond to HOMO/LUMO (T1, 57%) and HOMO/LUMO + 2 (T2, 62%) transitions. While the HOMO and the LUMO show dominating contributions of π-type molecular orbitals located on the phenolate ligand (HOMO) or the diaryl ligand (LUMO), the LUMO + 2 contains significant σ*(Bi–O) antibonding contributions, suggesting the possibility of photochemically-initiated Bi–O homolysis in **1-OPh**.

The catalytic dehydrocoupling of phenylsilane (**S1**) with TEMPO has recently been investigated as a model reaction for *thermally*-initiated radical reactions by Hill and Coles, using $[Mg(N(SiMe_3)_2)_2(thf)_2]$ and the isolable bismuth radical $[Bi(NON^{Dipp})]^{\bullet}$, respectively, as (pre-)catalysts ($NON^{Dipp} = [(NDippSiMe_2)_2O]^{2-}$, Dipp = 2,6-*i*Pr$_2$-C$_6H_3$).[24a,30] We have demonstrated that **1-SPh** catalyzes this reaction in a complementary *photochemically*-induced approach, thereby introducing well-defined molecular bismuth compounds to the field of homogeneous photochemically-induced catalysis.[24b] With **1-OPh** in hands, we set out to evaluate the catalytic activity of this compound in the dehydrocoupling of **S1** with TEMPO.

In the absence of a catalyst, the reaction of $PhSiH_3$ (**S1**) with one equivalent of TEMPO in benzene at ambient temperature gave only minor amounts of the coupling product $PhSiH_2$(OTEMP) (**P1**), when constantly irradiated with a Hg-vapor lamp (Table 2, entry 1). The product of a potential two-fold dehydrocoupling, $PhSiH(OTEMP)_2$ (**P1'**), was not detected. In the presence of 10 mol% of **1-OPh**, however, quantitative conversion of TEMPO with **S1** was observed to give **P1** (50%) and **P1'** (25%) according to ^{1}H NMR spectroscopy, along with the formation of H_2 as a stoichiometric by-product (entry 2). This is a slight improvement of the catalytic performance compared to previously reported **1-SPh** (entry 3)[24b] and demonstrates that the efficient bismuth-based photochemically-induced approach to dehydrocoupling reactions is not limited to bismuth thiolates.

Table 2. Bismuth species in the catalyzed dehydrocoupling reaction of TEMPO with $PhSiH_3$ (**S1**), *n*HexSiH_3 (**S2**) or Ph_2SiH_2 (**S3**).

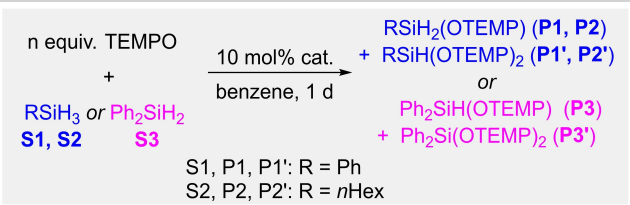

#	Cat.	Silane	n	Cond.	H_2 formation	Conversion [%][a]
1	none	**S1**	1	h·ν	no	10 (**P1**)
2	**1-OPh**	**S1**	1	h·ν	yes	>99 (50% **P1**, 25% **P1'**)
3[24b]	**1-SPh**	**S1**	1	h·ν	yes	93 (53% **P1**, 20% **P1'**)
4[24b]	**1-SPh**	**S1**	1	80 °C	no	3 (**P1**)
5	**1-OPh**	**S1**	1	80 °C	no	79 (55% **P1**, 12% **P1'**)
6[b]	**1-OPh**	**S1**	1	80 °C	no	33 (**P1**)[b]
7	**2**	**S1**	1	80 °C	no	6 (12% **P1**)
8	**3**	**S1**	1	80 °C	no	14 (14% **P1**)
9	**1-OPh**	**S2**	1	80 °C	no	19 (15% **P2**, 2% **P2'**)
10	**1-OPh**	**S2**	2	80 °C	no	11 (18% **P2**, 2% **P2'**)
11	**1-OPh**	**S3**	1	80 °C	no	71 (39% **P3**, 16% **P3'**)
12	**1-OPh**	**S3**	2	80 °C	no	38 (40% **P3**, 18% **P3'**)

[a] Conversion of TEMPO, determined by ^{1}H NMR spectroscopic analysis of silanes **S1**–**S3** and **P1**–**P3** (also see Supporting Information). [b] Conducted in silanized glass ware. *n*Hex = *n*-hexyl.

While unique reactivity patterns of bismuth compounds in stoichiometric dehydrocoupling reactions have been uncovered,[25c] the catalytic performance of bismuth compounds in *thermally*-initiated dehydrocoupling reactions has been moderate to poor so far.[24] For example, reaction of **S1** with TEMPO in the presence of 10 mol% of the isolable bismuth radical $[Bi(NON^{Dipp})]^{\bullet}$ led to the formation of 10% of **P1** after 1.7 d reaction time at 70 °C,[24a] and 10 mol% of **1-SPh** proved to be essentially inactive under similar conditions (1 d, 80 °C; entry 4).[24b] In contrast, 10 mol% of **1-OPh** led to 79% conversion of the substrate TEMPO, yielding the mono- and the disubstituted products **P1** and **P1'** (entry 5).[31] This is the first example of a thermally-initiated radical dehydrocoupling reaction that is effectively catalyzed by a bismuth compound. Importantly, the formation of the by-product H_2 is not observed during these reactions. This is in stark contrast to the reactions with **1-EPh** under *photochemical* conditions or with magnesium catalysts under thermal conditions, for which H_2 evolution has been reported.[24b,30] The formation or absence of H_2 in the course of these dehydrocoupling reactions indicates that different mechanistic scenarios are realized, depending on the choice of catalyst. I.e., different reaction pathways can be addressed with the catalyst **1-OPh** by applying either photochemical or thermal reaction conditions (entries 2 and 5). It should be noted that the formation of H_2 was suggested, when catalyst $[Bi(NON^{Dipp})]^{\bullet}$ was applied, but a resonance for H_2 is not visible in the ^{1}H NMR spectra of the reaction monitoring in the Supporting Information of this work; i.e. we suggest that a different mechanism may be operative here as well.[24a]

The lack of the formation of H_2 in the *thermal* approach with catalyst **1-OPh** raises the question of the fate of the hydrogen atoms. The elimination of benzene from a molecule containing an S–H and a Si–Ph moiety or from phenylsilane in the presence of a rare earth hydride complex have been reported.[32] This possibility could be ruled out, since no benzene was detected by ^{1}H NMR spectroscopy, when the reaction was performed in toluene under otherwise identical catalytic conditions (as in entry 5). Alternatively, TEMPO could act as a hydrogen atom acceptor to give TEMPO–H or the corresponding amine (2,2,6,6-tetramethylpiperidine) plus water. Their formation could not be unambiguously confirmed by ^{1}H NMR or IR spectroscopy (see Supporting Information). However, high-resolution mass spectrometric analysis of a standard catalytic reaction at 80 °C revealed a signal at *m/z* = 158.1536, indicating the formation of TEMPOH + H^+ during the reaction (this signal was not detected when analyzing a solution of pure TEMPO under identical conditions; see Supporting Information).[33] In addition, a catalytic experiment under standard conditions (entry 5) was also performed in previously silanized glassware, resulting in reduced yields of 33% (entry 6).[34] Thus, the substrate TEMPO and the surface of the glassware have been identified as being involved in providing hydrogen atom acceptors for the dehydrocoupling reaction, suggesting a complex mechanistic scenario in which parallel

Research Article
doi.org/10.1002/ejic.202100934

reaction pathways are likely to be operative. Two literature-known[24b] bismuth compounds, the "tempoxide" [Bi($C_6H_4CH_2$)$_2$S-(OTEMP)] (**2**) and the dibismuthane [Bi($C_6H_4CH_2$)$_2$S]$_2$ (**3**), could be detected as potential intermediates from standard catalytic reactions by ^{1}H NMR spectroscopy and single crystal X-ray diffraction analysis, respectively. Applying **2** as a catalyst in the *thermal* approach gave only low conversions, suggesting it is not directly involved in the main catalytic cycle (entry 7). Dibismuthane **3** as a catalyst leads to low, but significant conversions of **S1** (entry 8) and higher conversions may be possible, when **3** is generated *in situ*, because the isolated species shows a low solubility in benzene.[24b] These observations suggest **3** as a potential intermediate in the catalytic cycle.

Preliminary investigations into the substrate scope of the thermally-initiated dehydrocoupling of TEMPO with silanes show reduced catalytic activities for silanes bearing one alkyl substituent (*n*HexSiH$_3$ (**S2**), entries 9,10). However, in contrast to the *photochemically*-induced reaction with **1-SPh** as catalyst, using **1-OPh** in a *thermally*-initiated catalysis leads to good conversions of di(phenyl)silane (**S3**), and even the double substituted product (**P3'**) is observed in relevant yields (entries 11,12). Substitutions on tertiary (Ph$_3$SiH and Hex$_3$SiH) or sterically hindered secondary silanes (*t*Bu$_2$SiH$_2$) with TEMPO were not observed under the applied reaction conditions.

The polar character of the Bi–O bond and the relatively high natural charge at the bismuth atom of **1-OPh** prompted us to also investigate this compound as a catalyst in dehydrocoupling reactions of alcohols with silanes, which may be expected to follow a polar reaction pathway (Table 3). As a model reaction, the dehydrocoupling of phenylsilane (**S1**) with phenol (**S4**) was investigated. Under photochemical conditions, **1-OPh** as a catalyst led to low conversions (Table 3, entry 1). In contrast, 10 mol% of **1-OPh** as a catalyst led to quantitative conversion in the reaction of **S1** with two equivalents of **S4** in benzene at 80 °C in 1 d with a negligible background reaction (entries 2,3). Relevant conversions of 50% were observed for the less reactive secondary silane Ph$_2$SiH$_2$ (**S5**) (entry 4). While considerably more active catalysts for this type of reaction have been reported,[35] these results broaden the substrate scope of the bismuth-based catalyst and demonstrate its versatility in dehydrocoupling reactions.

In order to test for the involvement of radical species in these transformations, the reaction of phenylsilane with phenol in the presence of 10 mol% **1-OPh** was monitored by EPR spectroscopy at 80 °C for 24 h. Based on the absence of EPR spectroscopic resonances in these experiments, the involvement of persistent radical species was ruled out. At the same time, the formation of H_2 can be observed ^{1}H NMR spectroscopically in the thermally-induced dehydrocoupling reactions summarized in Table 3. Stoichiometric reaction between **1-OPh** with PhSiH$_3$ (**S1**) at 60 °C gives dibismuthane **3**, which was isolated as a red solid in near-quantitative yields. The use of **3** as a catalyst in the dehydrocoupling with phenol leads to low conversions of the starting materials – higher conversions are probably prevented by the poor solubility of the dibismuthane in benzene solution (*vide supra*; entry 5).

Table 3. Bismuth species in the catalyzed dehydrocoupling reaction of phenol (**S4**) with PhSiH$_3$ (**S1**) or Ph$_2$SiH$_2$ (**S3**).

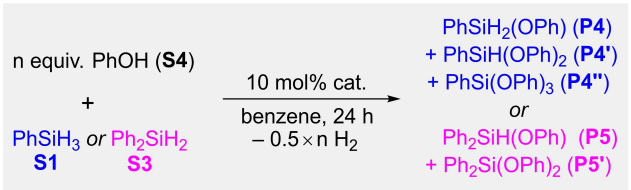

#	Cat.	Alc.	Silane	n	Cond.	Conversion [%][a]
1	**1-OPh**	**S4**	**S1**	1	h·ν	22 (7% **P4**, 6% **P4'**, 1% **P4''**)
2	none	**S4**	**S1**	2	80 °C	<1
3	**1-OPh**	**S4**	**S1**	2	80 °C	>99 (1% **P4**, 23% **P4'**, 51% **P4''**)
4	**1-OPh**	**S4**	**S3**	2	80 °C	50 (42% **P6**, 29% **P6'**)
5	**3**	**S4**	**S1**	2	80 °C	10 (8% **P4'**, 1% **P4''**)

[a] The conversion of **S4** was determined by NMR spectroscopy (Supporting Information).

Conclusions

In summary, the molecular di-organo(bismuth)alcoholate ($C_{14}H_{12}S$)Bi(EPh) (**1-OPh**, E = O) has been synthesized, isolated, and fully characterized, thereby completing the series of compounds **1-EPh** (E = O–Te). NMR and UV/Vis spectroscopy, in combination with (TD-)DFT calculations reveal a relatively polar Bi–O bond in **1-OPh**, which, however, remains susceptible to homolysis. Using simple dehydrocouplings between TEMPO or phenol and a range of silanes as model reactions, this unusual bonding situation was translated into catalytic scenarios. In contrast to previously reported main group catalysts for these reactions, **1-OPh** is active as a radical catalyst (with TEMPO as a substrate) under thermal *and* photochemical conditions, operating via different mechanisms (with and without the necessity for a hydrogen acceptor), *and* as a catalyst operating via polar reaction pathways (with phenol as a substrate). The versatility of the bismuth alcoholate catalyst opens up perspectives for future investigations towards switchable catalysis.

Experimental Section

General considerations. All air- and moisture-sensitive manipulations were carried out using standard vacuum line Schlenk techniques or in gloveboxes containing an atmosphere of purified argon (for details see the Supporting Information).

Synthesis of 1-OPh. Phenol (47.1 mg, 0.50 mmol) was added to a suspension of sodium hydride (12.0 mg, 0.50 mmol) in THF (1 mL) at 0 °C. The reaction mixture was stirred at 0 °C for 1 h, then for additional 45 min at ambient temperature. A solution of precursor [($C_{14}H_{12}S$)BiCl][36] (212 mg, 0.45 mmol) in THF (5 mL) was added dropwise at −78 °C. The suspension was stirred at −78 °C for 20 min, then at ambient temperature for 1 h 25 min. All volatiles were removed under reduced pressure and the residue was extracted with a benzene/THF (1:0.5, 2×3 mL) mixture and filtered. The filtrate was layered with *n*-pentane (6 mL). The product had precipitated as colorless crystals after 16 h at ambient temperature,

was isolated by filtration and dried *in vacuo*. Yield: 189 mg, 0.36 mmol, 79%.

^{1}H NMR (500 MHz, C_6D_6):[37] $\delta = 3.45$ (d, 2H, $^2J_{HH} = 15.4$ Hz, CH_2), 3.55 (d, 2H, $^2J_{HH} = 15.4$ Hz, CH_2), 6.91–7.02 (m, 5H, *para*-C_6H_5, H-4, H-8, H-3, H-9), 7.17 (m, 2H, *ortho*-C_6H_5, overlap with solvent resonance), 7.27 (ddd, 2H, $^4J_{HH} = 1.5$ Hz, $^3J_{HH} = 7.0$ Hz, $^3J_{HH} = 7.0$ Hz, H-2, H-10), 7.39 (m, 2H, *meta*-C_6H_5), 8.80 (d, 2H, $^3J_{HH} = 7.6$ Hz, H-1, H-11) ppm.

^{13}C{^{1}H} NMR (125.8 MHz, C_6D_6):[37] $\delta = 40.3$ (s, CH_2), 117.9 (s, *para*-C_6H_5), 121.1 (s, *ortho*-C_6H_5), 128.4 (s, C-3, C-9), 130.0 (s, *meta*-C_6H_5), 130.2 (s, C-2, C-10), 131.0 (s, C-4, C-8), 137.4 (s, C-1, C-11), 146.7 (s, C-4a, C-7a), 166.0 (s, *ipso*-C_6H_4), 176.8 (br, C-11a, C-12a) ppm.

Elemental analysis: Anal. calc. for: [$C_{20}H_{17}BiSO$] (514.39 g/mol): C 46.70, H 3.33, S 6.23; found: C 46.87, H 3.44, S, 6.27.

General procedure for catalytic coupling of TEMPO or phenol with silanes. In a J. Young-NMR tube, the substrate (typically 0.09 mmol) was dissolved in benzene-d_6 (0.5 mL). The desired amount (typically 10 mol%) of the selected catalyst and TEMPO or phenol (one or two equivalents, see Tables 2 and Table 3) were added, and the chosen reaction conditions were applied for the time noted in Tables 2 and Table 3. The conversion of TEMPO/phenol is given in these tables and was determined through NMR spectroscopic quantification of the silanes **S1**–**S3** and **P1**–**P5** in the reaction mixture. The reaction conditions used (as noted in Table 2 and Table 3) were either a photochemical set-up (constant irradiation with a mercury-vapor lamp at 23 °C (conditions: h·ν)) or the reaction was kept under ambient light at 80 °C (thermal approach). For further details, see the Supporting Information.

Deposition Number 2115890 (for **1-OPh**) contains the supplementary crystallographic data for this paper. These data are provided free of charge by the joint Cambridge Crystallographic Data Centre and Fachinformationszentrum Karlsruhe Access Structures service www.ccdc.cam.ac.uk/structures.

Acknowledgements

We thank Alexander Reckziegel and Dr. Gunnar Werncke for support in UV/vis analyses. Funding through the FCI, the Universitätsbund Würzburg, and the DFG (LI 2860/5-1) is gratefully acknowledged. This project has received funding from the European Research Council (ERC) under the European Union's Horizon 2020 research and innovation program (grant agreement No 946184). Open Access funding enabled and organized by Projekt DEAL.

Conflict of Interest

The authors declare no conflict of interest.

Data Availability Statement

The data that support the findings of this study are available in the supplementary material of this article.

Keywords: Bismuth · Catalysis · Chalcogens · Dehydrocoupling · Radical reactions

[1] a) T. Ollevier, *Org. Biomol. Chem.* **2013**, *11*, 2740–2755; b) J. M. Bothwell, S. W. Krabbe, R. Mohan, *Chem. Soc. Rev.* **2011**, *40*, 4649–4707; c) R. Mohan, N. Leonard, L. Wieland, *Tetrahedron* **2002**, *58*, 8373–8397.
[2] a) R. Qiu, Y. Qiu, S. Yin, X. Song, Z. Meng, X. Xu, X. Zhang, S. Luo, C.-T. Au, W.-Y. Wong, *Green Chem.* **2010**, *12*, 1767–1771; b) X. Zhang, S. Yin, R. Qiu, J. Xia, W. Dai, Z. Yu, C.-T. Au, W.-Y. Wong, *J. Organomet. Chem.* **2009**, *694*, 3559–3564.
[3] a) C. J. Carmalt, N. C. Norman, A. G. Orpen, S. E. Stratford, *J. Organomet. Chem.* **1993**, *460*, C22-C24; b) H. Dengel, C. Lichtenberg, *Chem. Eur. J.* **2016**, *22*, 18465–18475; c) M. Olaru, D. Duvinage, E. Lork, S. Mebs, J. Beckmann, *Angew. Chem. Int. Ed.* **2018**, *57*, 10080–10084; *Angew. Chem.* **2018**, *130*, 10237–10241; d) J. Ramler, K. Radacki, J. Abbenseth, C. Lichtenberg, *Dalton Trans.* **2020**, *49*, 9024–9034.
[4] C. Lichtenberg, *Chem. Commun.* **2021**, *57*, 4483–4495.
[5] a) S. Balasubramaniam, S. Kumar, A. P. Andrews, B. Varghese, E. D. Jemmis, A. Venugopal, *Eur. J. Inorg. Chem.* **2019**, *2019*, 3265–3269; b) R. Kannan, S. Balasubramaniam, S. Kumar, R. Chambenahalli, E. D. Jemmis, A. Venugopal, *Chem. Eur. J.* **2020**, *26*, 12717–12721; c) C. J. Carmalt, L. J. Farrugia, N. C. Norman, *J. Chem. Soc. Dalton Trans.* **1996**, 443–454.
[6] a) J. Ramler, C. Lichtenberg, *Chem. Eur. J.* **2020**, *26*, 10250–10258; b) J. Ramler, K. Hofmann, C. Lichtenberg, *Inorg. Chem.* **2020**, *59*, 3367–3376; c) R. Kannan, S. Kumar, A. P. Andrews, E. D. Jemmis, A. Venugopal, *Inorg. Chem.* **2017**, *56*, 9391–9395.
[7] a) *Category 1, Organometallics, Vol. 4*, 1st Edition ed., Georg Thieme Verlag, Stuttgart, **2002**; b) L. Dostál, *Coord. Chem. Rev.* **2017**, *353*, 142–158.
[8] a) R. J. Schwamm, J. R. Harmer, M. Lein, C. M. Fitchett, S. Granville, M. P. Coles, *Angew. Chem. Int. Ed.* **2015**, *54*, 10630–10633; *Angew. Chem.* **2015**, *127*, 10776–10779; b) C. Ganesamoorthy, C. Helling, C. Wölper, W. Frank, E. Bill, G. E. Cutsail, S. Schulz, *Nat. Commun.* **2018**, *9*, 87; c) C. Helling, S. Schulz, *Eur. J. Inorg. Chem.* **2020**, *2020*, 3209–3221; d) C. Lichtenberg, in *Encyclopedia of Inorganic and Bioinorganic Chemistry*, Wiley VCH, **2020**, pp. 1–12; e) G. E. Cutsail, *Dalton Trans.* **2020**, *49*, 12128–12135.
[9] a) G. Huttner, U. Weber, L. Zsolnai, *Z. Naturforsch.* **1982**, *37b*, 707–710; b) L. Xu, S. Bobev, J. El-Bahraoui, S. C. Sevov, *J. Am. Chem. Soc.* **2000**, *122*, 1838–1839.
[10] C. Lichtenberg, *Angew. Chem. Int. Ed.* **2016**, *55*, 484–486; *Angew. Chem.* **2016**, *128*, 494–496.
[11] D. P. Mukhopadhyay, D. Schleier, S. Wirsing, J. Ramler, D. Kaiser, E. Reusch, P. Hemberger, T. Preitschopf, I. Krummenacher, B. Engels, I. Fischer, C. Lichtenberg, *Chem. Sci.* **2020**, *11*, 7562–7568.
[12] S. Ishida, F. Hirakawa, K. Furukawa, K. Yoza, T. Iwamoto, *Angew. Chem. Int. Ed.* **2014**, *53*, 11172–11176; *Angew. Chem.* **2014**, *126*, 11354–11358.
[13] J. Ramler, F. Fantuzzi, F. Geist, A. Hanft, H. Braunschweig, B. Engels, C. Lichtenberg, *Angew. Chem. Int. Ed.* **2021**, DOI: doi.org/10.1002/anie.202109545.
[14] H. Qin, N. Yamagiwa, S. Matsunaga, M. Shibasaki, *J. Am. Chem. Soc.* **2006**, *128*, 1611–1614.
[15] R. Qiu, S. Yin, X. Zhang, J. Xia, X. Xu, S. Luo, *Chem. Commun.* **2009**, 4759–4761.
[16] G. Sabitha, E. V. Reddy, C. Maruthi, J. J. T. I. Yadav, *Tetrahedron Lett.* **2002**, *43*, 1573–1575.
[17] H. R. Kricheldorf, *Chem. Rev.* **2009**, *109*, 5579–5594.
[18] F. Wang, O. Planas, J. Cornella, *J. Am. Chem. Soc.* **2019**, *141*, 4235–4240.
[19] Y. Pang, M. Leutzsch, N. Nöthling, F. Katzenburg, J. Cornella, *J. Am. Chem. Soc.* **2021**, *143*, 12487–12493.
[20] O. Planas, F. Wang, M. Leutzsch, J. Cornella, *Science* **2020**, *367*, 313–317.
[21] C. Lichtenberg, *Chem. Eur. J.* **2020**, *26*, 9674–9687.
[22] a) S. Yamago, E. Kayahara, M. Kotani, B. Ray, Y. Kwak, A. Goto, T. Fukuda, *Angew. Chem. Int. Ed.* **2007**, *46*, 1304–1306; *Angew. Chem.* **2007**, *119*, 1326–1328; b) E. Kayahara, S. Yamago, *J. Am. Chem. Soc.* **2009**, *131*, 2508–2513; c) C. Lichtenberg, F. Pan, T. P. Spaniol, U. Englert, J. Okuda, *Angew. Chem. Int. Ed.* **2012**, *51*, 13011–13015; *Angew. Chem.* **2012**, *124*, 13186–13190.
[23] a) J. Ramler, I. Krummenacher, C. Lichtenberg, *Angew. Chem. Int. Ed.* **2019**, *58*, 12924–12929; *Angew. Chem.* **2019**, *131*, 13056–13062; b) J. Ramler, C. Lichtenberg, *Dalton Trans.* **2021**, *50*, 7120–7138.
[24] a) R. Schwamm, M. Lein, M. Coles, C. Fitchett, *Chem. Commun.* **2018**, *54*, 916–919; b) J. Ramler, I. Krummenacher, C. Lichtenberg, *Chem. Eur. J.* **2020**, *26*, 14551–14555.
[25] a) L. H. Long, J. F. Sackman, *Trans. Faraday Soc.* **1954**, *50*, 1177–1182; b) T. A. Hanna, A. L. Rieger, P. H. Rieger, X. Wang, *Inorg. Chem.* **2002**, *41*, 3590–3592; c) K. Oberdorf, A. Hanft, J. Ramler, I. Krummenacher, F. M.

Bickelhaupt, J. Poater, C. Lichtenberg, *Angew. Chem. Int. Ed.* **2021**, *60*, 6441–6445; *Angew. Chem.* **2021**, *133*, 6513–6518.
[26] a) V. Blanco, D. A. Leigh, V. Marcos, *Chem. Soc. Rev.* **2015**, *44*, 5341–5370; b) H. A. Houck, F. E. Du Prez, C. Barner-Kowollik, *Nat. Commun.* **2017**, *8*, 1869; c) B. M. Neilson, C. W. Bielawski, *ACS Catal.* **2013**, *3*, 1874–1885.
[27] a) I. J. Casely, J. W. Ziller, B. J. Mincher, W. J. Evans, *Inorg. Chem.* **2011**, *50*, 1513–1520; b) S.-F. Yin, J. Maruyama, T. Yamashita, S. Shimada, *Angew. Chem. Int. Ed.* **2008**, *47*, 6590–6593; *Angew. Chem.* **2008**, *120*, 6692–6695; c) S. Yoshida, M. Yasui, F. Iwasaki, Y. Yamamoto, X. Chen, K. Akiba, *Acta Crystallogr. Sect. B* **1994**, *50*, 151–157; d) Y. Yamamoto, X. Chen, K. Akiba, *J. Am. Chem. Soc.* **1992**, *114*, 7906–7907; e) X. Chen, Y. Yamamoto, K.-Y. Akiba, *Heteroat. Chem.* **1995**, *6*, 293–303.
[28] a) J. P. H. Charmant, A. G. Orpen, S. C. James, N. C. Norman, J. Starbuck, *Acta Crystallogr. Sect. E* **2002**, *58*, m488–m489; b) R. Hillwig, F. Kunkel, K. Harms, B. Neumüller, K. Dehnicke, *Zeitsch. Naturforsch. B* **1997**, *52*, 149–152.
[29] a) For comparison with series of diorgano bismuth compounds containing $(EPh)^-$ ligands (E = S, Se, Te), see: ; b) F. Calderazzo, A. Morvillo, G. Pelizzi, R. Poli, F. Ungari, *Inorg. Chem.* **1988**, *27*, 3730–3733; c) P. Simon, R. Jambor, A. Ruzicka, L. Dostal, *Organometallics* **2013**, *32*, 239–248.
[30] D. J. Liptrot, P. M. S. Hill, M. F. Mahon, *Angew. Chem. Int. Ed.* **2014**, *53*, 6224–6227; *Angew. Chem.* **2014**, *126*, 6338–6341.
[31] Changing the molar ratio of the substrates TEMPO and S1 from 1:1 to 2:1 did not increase the conversion and the product distribution (**P1** vs **P1'**) was virtually unaffected.
[32] a) N. Fontana, N. A. Espinosa-Jalapa, M. Seidl, J. O. Bauer, *Chem. Eur. J.* **2021**, *27*, 2649–2653; b) I. Castillo, T. D. Tilley, *Organometallics* **2001**, *20*, 5598–5605.
[33] For examples TEMPO acting as a hydrogen atom acceptor see: a) T. Gunasekara, G. P. Abramo, A. Hansen, H. Neugebauer, M. Bursch, S. Grimme, J. R. Norton, *J. Am. Chem. Soc.* **2019**, *141*, 1882–1886; b) A. Baschieri, L. Valgimigli, S. Gabbanini, G. A. DiLabio, E. Romero-Montalvo, R. Amorati, *J. Am. Chem. Soc.* **2018**, *140*, 10354–10362.
[34] For examples of reactions being influenced by the surfaces and studies on the interaction of hydrogen atoms with glass surfaces see: a) Y. Li, T. F. Mehari, Z. Wei, Y. Liu, R. G. Cooks, *Angew. Chem. Int. Ed.* **2021**, *60*, 2929–2933; *Angew. Chem.* **2021**, *133*, 2965–2969; b) Y. Li, K.-H. Huang, N. M. Morato, R. G. Cooks, *Chem. Sci.* **2021**, *12*, 9816–9822; c) D. B. Sheen, *J. Chem. Soc. Faraday Trans. 1* **1979**, *75*, 2439–2453; d) T. W. Hickmott, *J. Appl. Phys.* **1960**, *31*, 128–136; e) A. M. Filbert, M. L. Hair, in *Advances in Corrosion Science and Technology: Volume 5* (Eds.: M. G. Fontana, R. W. Staehle), Springer US, Boston, MA, **1976**, pp. 1–54.
[35] a) J. M. Blackwell, K. L. Foster, V. H. Beck, W. E. Piers, *J. Org. Chem.* **1999**, *64*, 4887–4892; b) W. Sattler, G. Parkin, *J. Am. Chem. Soc.* **2012**, *134*, 17462–17465; c) D. Mukherjee, R. R. Thompson, A. Ellern, A. D. Sadow, *ACS Catal.* **2011**, *1*, 698–702; d) L. J. Morris, M. S. Hill, M. F. Mahon, I. Manners, F. S. McMenamy, G. R. Whittell, *Chem. Eur. J.* **2020**, *26*, 2954–2966.
[36] X.-W. Zhang, J. Xia, H.-W. Yan, S.-L. Luo, S.-F. Yin, C.-T. Au, W.-Y. Wong, *J. Organomet. Chem.* **2009**, *694*, 3019–3026.
[37] The assignment of ^{1}H and ^{13}C NMR spectroscopic resonances of compound **1-OPh** was performed according to the labelling scheme shown in Figure S1 (Supporting Information).

Manuscript received: October 29, 2021
Revised manuscript received: November 23, 2021
Accepted manuscript online: November 24, 2021